Published in final edited form as:
Dev Biol. 2008 April 15; 316(2): 383–396.

misty somites, a maternal effect gene identified by transposon-mediated insertional mutagenesis in zebrafish that is essential for the somite boundary maintenance

Tomoya Kotani[a,†] and **Koichi Kawakami**[a,b,*]

a *Division of Molecular and Developmental Biology, National Institute of Genetics, 1111 Yata, Mishima, Shizuoka 411-8540, Japan*

b *Department of Genetics, The Graduate University for Advanced Studies (SOKENDAI), 1111 Yata, Mishima, Shizuoka 411-8540, Japan*

Abstract

Somite boundary formation is crucial for segmentation of vertebrate somites and vertebrae and skeletal muscle morphogenesis. Previously, we developed a *Tol2* transposon-mediated gene trap method in zebrafish. In the present study, we aimed to isolate transposon insertions that trap maternally-expressed genes. We found that homozygous female fish carrying a transposon insertion within a maternally-expressed gene *misty somites* (*mys*) produced embryos that showed obscure somite boundaries at the early segmentation stage (12–13 hpf). The somite boundaries became clear and distinct after this period and the embryos survived to adulthood. This phenotype was rescued by expression of *mys* cDNA in the homozygous adults, confirming that it was caused by a decreased *mys* activity. We analyzed a role of the *mys* gene by using morpholino oligonucleotides (MOs). The MO-injected embryo exhibited severer phenotypes than the insertional mutant probably because the *mys* gene was partially active in the insertional mutant. The MO-injected embryo also showed the obscure somite boundary phenotype. Fibronectin and phosphorylated FAK at the intersomitic regions were accumulated at the boundaries at this stage, but, unlike wild type embryos, somitic cells adjacent to the boundaries did not undergo epithelialization, suggesting that Mys is required for epithelialiation of the somitic cells. Then in the MO-injected embryos, the boundaries once became clear and distinct, but, in the subsequent stages, disappeared, resulting in abnormal muscle morphogenesis. Accumulation of Fibronectin and phosphorylated FAK observed in the initial stage also disappeared. Thus, Mys is crucial for maintenance of the somite boundaries formed at the initial stage. To analyze the *mys* defect at the cellular level, we placed cells dissociated from the MO-injected embryo on Fibronectin-coated glasses. By this cell spreading assay, we found that the *mys*-deficient cells reduced the activity to form lamellipodia on Fibronectin while FAK was activated in these cells. Thus, we demonstrate that a novel gene *misty somites* is essential for epithlialization of the somitic cells and maintenance of the somite boundary. Furthermore, Mys may play a role in a cellular pathway leading to lamellipodia formation in response to the Fibronectin signaling. We propose that the *Tol2* transposon mediated gene trap method is powerful to identify a novel gene involved in vertebrate development.

*Corresponding author. Fax: +81 55 981 5827., E-mail address: kokawaka@lab.nig.ac.jp (K. Kawakami).
†Present address: Laboratory of Molecular and Cellular Interactions, Faculty of Advanced Life Science, Hokkaido University, Sapporo 060-0810, Japan.

Introduction

Somites are morphologically distinct segmental units that are transiently formed during vertebrate embryogenesis and give rise to metameric and fundamental structures such as the vertebrate axial skeleton and their associated muscles. The reiterative pattern of the somite is formed from the anterior to the posterior by a mechanism so-called segmentation clock (Pourquie, 2003). The morphologically distinct boundaries are formed in the intersomitic regions and the somitic cells undergo gross morphological changes to yield the sclerotome, myotome and dermatome (Keynes and Stern, 1988).

In a model vertebrate zebrafish, most somitic cells give rise to muscle fibers. Somitic cells on both side of the intersegmental boundaries undergo a mesenchymal-to-epithelial transition and then elongate to form long muscle fibers that are anchored to the boundaries (Devoto et al., 1996; Stickney et al., 2000). Henry et al. defined three stages of the somite boundary formation (Henry et al., 2005). The first stage is the formation of the initial epithelial boundaries that involves accumulation of the extracellular matrix (ECM) components at the intersomitic regions. Fibronectin is a major component of ECM that promotes cell adhesion, cell migration and cytoskeletal organization. During the initial boundary formation, Fibronectin is localized to the intersomitic regions (Crawford et al., 2003). The focal adhesion kinase (FAK) is activated through Fibronectin-Integrin signaling (Burridge et al., 1992; Guan and Shalloway, 1992). At this stage, phosphorylated FAK (an active form of FAK) is also localized at the boundaries (Crawford et al., 2003; Henry et al., 2001). The second stage is a transition stage from the initial somite boundary formation to the myotome boundary formation. The boundaries become chevron-shaped, and muscle precursor cells begin to elongate. The third stage is the formation of the myotome boundary. At this stage, all muscle precursor cells fully elongate to generate the myotome. The myotome boundaries are exceedingly rich in ECM components and phosphorylated FAK. The boundaries that were formed at the first stage are maintained through the later stages.

Zebrafish is an excellent model animal to identify developmental genes by forward genetics approaches. Large-scale mutagenesis screens by using a chemical mutagen ENU have identified zygotic mutations that affect early somitogenesis (Julich et al., 2005a; Koshida et al., 2005; van Eeden et al., 1996). Studies of these mutants have revealed that genes involved in the Notch pathway; *after eight*/*deltaD* (Holley et al., 2000), *deadly seven*/*notch1a* (Holley et al., 2002), *mind bomb* (E3 ubiquitin ligase) (Itoh et al., 2003) and *beamter*/*deltaC* (Julich et al., 2005b), genes involved in the Fibronectin-Integrin signaling pathway; *integrinα5* and *fibronectin* (Julich et al., 2005a; Koshida et al., 2005), and *fused somites*/*tbx24* (Nikaido et al., 2002) are crucial for somitogenesis. Although these mutants show different types of defects in the somite boundary formation, namely the Notch pathway mutants are defective in the posterior somites, the Fibronectin-Integrin pathway mutants are defective in the anterior somites and the *tbx24* mutant is defective in both anterior and posterior somites, all of them showed defects during the formation of the initial epithelial boundary formation, the first stage of the somite boundary formation defined by Henry et al. (Henry et al., 2005). Thus, little is known about genes involved in the maintenance of the epithelial boundaries through the transition and myotome boundary formation stages.

The large-scale chemical mutagenesis screens in zebrafish have estimated that only 2,400 genes are zygotically essential (Driever et al., 1996; Haffter et al., 1996) although there may be 30,000 or more genes in the zebrafish genome. Also a large-scale insertional mutagenesis screen using a pseudotyped retrovirus has estimated that the zebrafish genome contains only 1,400 zygotically essential genes (Amsterdam et al., 2004). On the other hand, chemical mutagenesis screens for maternal effect mutants have been carried out, and it was shown that maternal factors also regulate various developmental processes as well as zygotic factors (Dosch et al.,

2004; Kishimoto et al., 2004; Pelegri et al., 1999; Wagner et al., 2004). These maternal effect mutants should be valuable sources to discover novel genes that had not been discovered by the zygotic screens. Identification of mutated genes however are laborious and time-consuming, especially for maternal mutations, since it requires genetic mapping and positional cloning.

We have developed the transposon-mediated transgenesis method in zebrafish by using the medaka fish *Tol2* transposable element (Kawakami et al., 1998; Kawakami and Shima, 1999; Kawakami et al., 2000). Recently, we have successfully performed a gene trap screen by using the *Tol2* transposon system and created a number of fish expressing GFP in temporally and spatially restricted patterns (Kawakami et al., 2004). In these fish, insertions of the gene trap transposon construct captured endogenous transcripts and interfered with their normal splicing partially or nearly completely (Kawakami et al., 2004; Kotani et al., 2006), suggesting that the gene trap method is applicable to insertional mutagenesis. In this study, we aimed to isolate maternal effect mutants by performing the *Tol2*-mediated gene trap approach. We hypothesized that, if the gene trap construct was integrated in maternally expressed genes, GFP expression should be detected in fertilized eggs. Therefore, we "prescreened" insertions for GFP expression at the one cell stage, and created female fish homozygous for such insertions. Then we crossed these female fish and analyzed their progeny for developmental phenotypes. By this strategy, we isolated a maternal effect mutant, *misty somites*. We will describe the identification and characterization of a novel gene, *misty somites*, and the discovery of its role in maintenance of the initial epithelial somite boundary.

Materials and methods

Fish

SAG14A, SAG20A, SAG86A, SAGm11A, SAGm11B, SAGm18B, SAGp4A and SAGp53B, were isolated previously (Kawakami et al., 2004). SAGm11C, SAGm11D and SAGm11E were newly identified during outcrosses of SAGm11A and SAGm11B (Kawakami, 2005). SAGn10A, SAGn15C, SAGn25A and SAGn28C were created in this study. GFP expression was analyzed under a fluorescent stereoscope MZ 16 FA (Leica). Photos were taken by using DFC300FX (Leica). TL, Tuebingen (Tu) and TAB, a hybrid between Tu and AB were used as wild type fish.

Primers, Southern blot hybridization, inverse PCR, linker-mediated PCR, 5′RACE, 3′ RACE and RT-PCR

Primers used in this study are shown in Table S1. Southern blot hybridization, inverse PCR, linker-mediated PCR, 5′ RACE, 3′ RACE and RT-PCR were carried out as described previously (Kawakami, 2004;Kawakami et al., 2004;Kotani et al., 2006). The PCR products were purified from a gel or cloned by TA cloning kit (Invitrogen), and sequenced by using BigDye Terminator v3.1 Cycle sequencing kit (Applied Biosystems) and ABI PRISM 3130xl Genetic Analyzer (Applied Biosystem). OligodT30 Super mRNA Purification Kit (Takara) was used to purify poly(A)$^+$ RNA.

Construction of Tol2-mys transgenic fish

1305 bp of cDNA containing the open reading frame for the Mys protein was amplified by RT-PCR using *mys*-f1-ATG and *mys*-r9, and cloned between the *Bam*HI and *Cla*I sites of T2KXIG in (Urasaki et al., 2006), resulting in *Tol2-mys*. Four fish injected with a plasmid containing *Tol2-mys* and the transposase mRNA were crossed with SAG20A homozygous fish and 50 embryos from each cross were pooled and analyzed by PCR. Three fish transmitted *Tol2-mys* to the progeny. Then 130 F1 fish from one of three founder fish were raised and analyzed by PCR and Southern blot analysis. One female that carried a single copy insertion

of *Tol2-mys* was identified. Since the transposase mRNA was injected, it is possible that the SAG20A insertion had been mobilized. To avoid this possibility, we performed PCR and confirmed that the fish was indeed homozygous for the SAG20A insertion.

Anti-mys MOs and flag-mys RNA

The sequences of antisense molpholino oligonucleotides (MOs) (Gene Tools, LLC) are shown in Table S1. ATG-MO hybridizes to the translational initiation site. 5-mis-ATG-MO contains 5-bp mismatches around the ATG codon and was used as control. 2SD-MO and 4SD-MO hybridize to the splice donors of the second and forth exon, respectively. MOs were suspended in H_2O and injected by using Femtojet (Eppendorf). Oligonucleotides encoding the Flag epitope tag and the Mys open reading frame were cloned into pCS2+, resulting in the Flag-Mys fusion protein that contained the Flag tag at the NH_2-terminus of Mys. *flag-mys* mRNA was synthesized with mMESSAGE mMACHINE SP6 Kit (Ambion Inc.). 1 nl of a solution containing 200 μg/ml mRNA was injected into fertilized eggs.

In situ hybridization and immunostaining

In situ hybridization experiments were performed as described (Schulte-Merker et al., 1992). For immunostaining, monoclonal anti-γ-Tubulin antibody (GTU-88, Sigma) (1:1000 dilution), polyclonal anti-Fibronectin antibody (Fibronectin Ab-10, NeoMarkers) (1:500 dilution), polyclonal anti-FAK [pY397] phosphospecific antibody (BioSource International) (1:200 dilution), polyclonal anti-Laminin antibody (Laminin Ab-1, Neomarkers) (1:100 dilution), monoclonal anti-Flag antibody (M2, Sigma) (1:500 dilution) and monoclonal anti-myosin heavy chain antibody (S58, Developmental Studies Hybridoma Bank) (1:20 dilution) were used. Embryos were fixed in 4% PFA/PBS for overnight at room temperature (for Fibronectin, phosphorylated FAK, Laminin and Flag-Mys) or fixed in Carnoy's fixative for 20 min at room temperature (for S58), treated with 0.5% Tween 20/PBS at room temperature for 1.5 hr or with acetone at −20 C for 5 min (for γ-Tubulin), rinsed with PBS, incubated in 2% BSA;10% DMSO; 0.2% Tween 20/PBS, and then incubated with the antibody at 4 °C for overnight. After washing with 0.2% Tween 20/PBS, the embryos were incubated with Alexa 488 or 546 goat anti-rabbit Ig antibody and Alexa 488 or 546 anti-mouse Ig (1:250 dilution) antibody (Molecular Probes) at 4 C for overnight. Alexa 488 or 546-phalloidin (Molecular Probes) was used at a 1:100 dilution at room temperature for 30 min to detect F-actin. 25 μg/ml propidium iodide was used at room temperature for 15 min to detect nuclei. The samples were observed under LSM5LIVE confocal laser scanning microscopy (Zeiss).

Cell Transplantation

Cell transplantation experiments were performed as described previously (Kishimoto et al., 1997). Donor embryos were injected at the one-cell stage with 1 nl of a mixture containing 2.5 μg/ml rhodamine-dextran (Molecular Probes) and 50 μg/ml GFP mRNA with or without 8 mg/ml ATG-MO. At the sphere stage, 10–20 cells were taken from an injected donor embryo and transplanted into a host embryo. Host embryos were fixed at 20 hpf and processed for staining as described above.

Cell spreading assay

Embryos obtained from the *mys* homozygous parents were injected with 1 nl of 4 mg/ml ATG-MO and 2.5 μg/ml rhodamine-dextran (Molecular Probes) at the one-cell stage. As a control, wild type embryos were injected only with rhodamine-dextran. The embryos were dechorionated at 4 hpf and transferred to DMEM medium (Sigma) containing 0.3 mg/ml L-glutamine, 100 U/ml penicillin and 0.1 mg/ml streptomycin (Montero et al., 2003), and were dissociated into single cells by pipetting. The dissociated cells were incubated on Fibronectin-coated slide glass (BD Biosciences) for overnight (~16 h) at 28 C. Then the cells were washed

three times with PBS, covered with PBS and analyzed under a fluorescent microscope Axio Imager Z1 (Zeiss). The photos were taken using AxioCam MRc5 (Zeiss). For immunostaining, the cells were fixed in 4% PFA/PBS for 1h at room temperature, incubated with the anti-FAK [pY397] antibody (1:200 dilution) and Alexa 633 goat anti-rabbit IgG antibody (Molecular Probes) (1:250 dilution) and analyzed by LSM5LIVE confocal laser scanning microscopy.

Results

Identification of a maternal mutant misty somites by the transposon-mediated gene trap approach

To identify maternal-effect mutants in zebrafish, we designed a novel screen based on transposon-mediated gene trapping (Fig. 1A–C). Previously, we developed a gene trap method by using the gene trap construct T2KSAG, which contained a splice accepter, promoter-less GFP and the polyA signal. We created random insertions of T2KSAG and identified 38 lines that expressed GFP in spatially and temporally restricted patterns (Kawakami et al., 2004; Kotani et al., 2006). We further created new gene trap lines, and established a total of 74 fish lines that expressed GFP in unique patterns.

First, we found that 34 out of 74 lines (46 %) expressed GFP at the one-cell stage. We hypothesized that, in these fish, T2KSAG was integrated within maternally expressed genes and captured their transcripts (Fig. 1A). Second, we cloned genomic DNA surrounding the integration sites, designed PCR primers that hybridized to genomic sequences flanking the transposon insertions, and identified homozygous fish by PCR (Fig. 1B). We thus established 15 homozygous fish lines carrying single copy insertions of T2KSAG. These homozygous fish were viable and fertile. We performed 5′ RACE for all of these 15 insertions (see supplementary information, Table S2). In 11 out of 15 cases, the trapped exons were identified. In four cases (SAGm11B, SAGm11D, SAGn15C and SAGn28C), the 5′ end was mapped within the T2KSAG sequence. We infer that, in these four cases, a cryptic promoter on T2KSAG may have been activated by chromosomal enhancers. Finally, we crossed homozygous females with wild type males, and analyzed the progeny (Figure 1C). We found that 100 % (183/183) of embryos produced from an SAG20A homozygous female formed obscure somite boundaries at the 3- and 6-somite stage (12 and 13 hpf) while embryos from wild type fish formed distinct somite boundaries at these stages (Fig. 1D). The somite boundaries in these embryos however became clear and distinct at the 14-somite stage.

Three SAG20A homozygous females identified in the sibling and SAG20A homozygous females identified in the next generation caused the same phenotype in their progeny, indicating the maternal phenotype was inheritable. Therefore, we named the maternal mutation *misty somites* (*mys*). Zygotically homozygous embryos did not show any obvious developmental phenotypes. We further crossed homozygous male and female fish and analyzed the progeny. The phenotypes of maternal and maternal-zygotic embryos are indistinguishable. Also in these homozygous adults, we did not observe skeletal defects as have been observed for other somite mutants (van Eeden et al., 1996).

Identification and expression of the mys gene

The SAG20A insertion was located in the first intron of a predicted gene. A 5′ RACE analysis detected a fusion transcript of the first exon of the predicted gene and the GFP gene. We further performed RT-PCR and 3′ RACE and confirmed that the predicted gene was indeed transcribed (Fig. 2A). The full-length transcript was 2380-bp, and had a capacity to encode a protein of 435 amino acids. We named the gene *misty somites* (*mys*) (GenBank accession: AB307684). Although no significant motif was detected in the amino acid sequence, highly conserved Mys protein homologs are found in other vertebrate genomes; in *Xenopus tropicalis* (GenBank

number: CAJ82347.1; 86% identity), in *Mus musculus* (NP_082723.1; 84% identity), in *Homo sapiens* (NP_570721.1; 84% identity), and in *Gallus gallus* (NP_001026588.1; 82% identity) (Fig. 2B). No obvious counterpart was detected in invertebrates.

In the SAG20A line, GFP was expressed maternally. When we crossed an SAG20A heterozygous female and a wild type male, all of the progeny showed strong GFP expression in the whole body at the one-cell stage and at 12 hpf (Fig. 2C, D). To analyze the zygotic expression, we crossed an SAG20A heterozygous male and a wild type female. In the progeny, weak GFP expression was detected in the whole body at the 3-somite stage (12 hpf) (Fig. 2E) and strong GFP expression was detected in the notochord at 24 hpf (Fig. 2M). In situ hybridization using the *gfp* probe also showed similar expression patterns (Fig. 2F–H). In consistent with the *gfp* expression, in situ hybridization detected the *mys* expression in the one cell stage embryo (Fig. 2I), in the whole body at 8 hpf (Fig. 2J), in the notochord and weakly and diffusely in the paraxial mesoderm at 13 hpf (Fig. 2K, L), and in the notochord and weakly in the whole body at 23 hpf (Fig. 2N).

To determine whether the insertion abolished the *mys* transcript, we analyzed SAG20A heterozygous and homozygous embryos by RT-PCR (Fig. 2O). The homozygous embryos were obtained from homozygous parents. RT-PCR using f1 and r7 did not amplify a PCR product from homozygous embryos (Fig. 2O, top), indicating that the insertion blocked synthesis of mRNA containing the first and second exons nearly completely. We then performed RT-PCR using f2 and r7 to determine whether mRNA containing exons downstream of the second exon was synthesized in the homozygous embryos. A faint band was detected (Fig. 2O, middle). We performed 5′ RACE using poly(A)+ RNA and mapped the 5′ end of this transcript within the first intron, 556-bp upstream of the splice donor of the second exon. Since the initiator ATG codon of the *mys* gene is encoded by the second exon, it is possible that the Mys protein may be synthesized at low levels in the homozygous fish.

Rescue of the mys mutant by transgenesis

To determine whether the *mys* gene is indeed responsible for the mutant phenotype, we performed a rescue experiment by transgenesis. We constructed the *Tol2-mys* construct containing cloned *mys* cDNA under the control of *Xenopus* EF1 α promoter that can direct maternal expression as well as ubiquitous expression (Fig. 3A). It is expected that the Mys protein can be supplied from this construct as a maternal factor. We co-injected a transposon-donor plasmid containing *Tol2-mys* and the transposase mRNA into fertilized eggs obtained from SAG20A homozygous parents. The injected fish were raised and crossed with SAG20A homozygous fish, and the progeny that were homozygous for the SAG20A insertion and heterozygous for a single copy insertion of *Tol2-mys* were identified. Then, we crossed the double transgenic female with a wild type male, and analyzed their progeny for the somite boundary phenotype (Fig. 3B). Unlike the progeny from SAG20A homozygous female (Fig. 3C), all of them (178/178) showed normal somite boundaries at 13 hpf (Fig. 3D), indicating the mutant phenotype was rescued by expression of the *mys* cDNA. Therefore we concluded that a decreased *mys* activity by the insertion of T2KSAG is the cause of the observed mutant phenotype.

Inhibition of the mys activity caused defects in the somite boundary formation

Since we found that the *mys* gene may be partially active in the homozygous fish, we aimed to knock down the *mys* activity more severely by using antisense morpholino oligonucleotide (MO). We injected ATG-MO into wild type embryos and found that the injected embryos showed a curved body phenotype at 26 hpf (Fig. 4A–C). Embryos injected with a control 5-mis-ATG-MO that contained 5-bp mismatches around the ATG codon did not show such a phenotype. In addition to the curved body phenotype, we found that in the ATG-MO injected

embryos the somite boundaries disappeared at 26 hpf (Fig. 4C). We counted embryos with only the curved body phenotype as class I, and embryos that showed both the curved body phenotype and the somite boundary disappearance as class II. We identified the class I phenotype in 16, 79 and 0 % of the embryos, and the class II phenotype in 0, 12 and 100 % of the embryos injected with 2, 4 and 8 ng of ATG-MO, respectively (Table 1). The obscure somite boundary phenotype at the 6-somite stage (13 hpf) was also observed in both class I and class II embryos (Fig. 4J). In the class II embryos, the somite boundaries once became clear and distinct at around the 14-somite stage (16 hpf) and then disappeared by the 21-somite stage (20 hpf) (Fig. 4J–N). We injected ATG-MO into embryos produced from homozygous *mys* parents. 5 and 93 % of embryos injected with 2 and 4 ng of ATG-MO, respectively, showed the class II phenotype (Fig. 4D and Table 1). Thus, the *mys* insertional mutation and the ATG-MO injection synergistically increased the severity of the phenotype, indicating that they were caused by specific inhibition of the *mys* activity but not by non-specific toxic effects due to MO injection.

Maternal mys activity plays a role in the somite boundary formation

Injection of ATG-MO is thought to block both maternal and zygotic *mys* activities. To determine how the zygotic *mys* activity contributed to the observed defects, we designed 2SD-MO that hybridized to the splice donor of the second exon (Fig. 4O). It is expected that SD-MO does not affect existing maternal *mys* mRNA but block splicing of zygotically transcribed *mys* mRNA. Injection of 8 ng of 2SD-MO into wild type embryos caused the curved body phenotype but did not cause either the obscure somite phenotype at 13 hpf or the somite boundary disappearance at 20 hpf (n=164; Fig. 4P, Q), suggesting that inhibition of the zygotic *mys* activity caused the class I phenotype. We analyzed the *mys* transcript in the 2SD-MO injected embryos by RT-PCR using f1 and r3. A band containing the second exon was amplified from the 2SD-MO injected embryos at 4 hpf, but not at 36 hpf. Instead, a band of a smaller size was amplified (Fig. 4T). This smaller product contained a transcript that skipped the second exon (data not shown), indicating that injection of 2SD-MO interfered with normal splicing of the zygotic transcript. Since the *mys* gene has an ATG codon in the third exon, it is still possible that the Mys protein lacking N-terminal 67 amino acids is synthesized in the 2SD-MO injected embryos. To exclude this possibility, we injected 16 ng of 4SD-MO that hybridized to the splice donor of the forth exon (Fig. 4O) into wild type embryos. Injection of 4SD-MO caused the class I phenotype but not the class II phenotype (n=182; Fig. 4R–S) as well as injection of 2SD-MO. RT-PCR using f3 and r7 detected a normally spliced transcript in the 4SD-MO injected embryos at 4 hpf, but not at 36 hpf. Instead, a band of a slightly larger size was amplified (Fig. 4U). This larger product contained 78-bp intronic sequences upstream of the forth exon, creating an in-frame stop codon, and therefore encoded a truncated Mys protein. These results indicate that inhibition of the zygotic *mys* activity cause the curved body phenotype but not the defects in the somite boundary. Further, we injected SD-MOs into the *mys* mutant embryos and found that the somite defects were not enhanced (data not shown).

The mys-deficiency impaired epithelialization of the somitic cells

We analyzed the ATG-MO injected embryos by whole mount in situ hybridization using the *fgf8* (Reifers et al., 1998), *deltaC* (Julich et al., 2005b), *mespb* (Sawada et al., 2000), *tbx24* (Nikaido et al., 2002) and *her13.2* (Kawamura et al., 2005) probes. These genes are involved in early somitogenesis. Expression of these mRNA were normal in the *mys*-deficient embryos (data not shown), suggesting that Mys is not involved in the early segmentation processes.

In the ATG-MO injected embryos, the somite boundaries were obscure at 13 hpf, became clear and distinct at 16 hpf, and then disappeared by 20 hpf. To analyze the morphology of the somite at 13 to 16 hpf in more detail, we performed immunostaining using the anti-γ-Tubulin antibody. The embryos were stained also with phalloidin. In the wild type embryos, cells adjacent to the

somite boundaries showed epithelial cell characteristics at 13 hpf and 16 hpf, i.e., a columnar shape and apical localization of the centrosome (Fig. 5A, C) (Barrios et al., 2003). In contrast, in the ATG-MO injected embryos at 13 hpf, the boundaries were unclear and cells located adjacent to the presumptive boundaries did not form the columnar shape. In these cells, the centrosomes were distributed randomly in the cytoplasm (Fig. 5B). At 16 hpf, the somite boundaries became clear and distinct, but the adjacent cells still did not form the columnar shape and the centrosomes were distributed randomly (Fig. 5D). These results suggest that Mys is required for epithelialization of the somitic cells adjacent to the boundaries.

Disappearance of the somite boundaries in the mys-deficient embryo

To analyze the morphology of the somite in the subsequent stages, we performed immunostaining using the anti-Fibronectin, anti-phosphorylated FAK and anti-Laminin antibodies. The embryos were stained also with phalloidin. Fibronectin and phosphorylated FAK were detected at the somite boundaries in both wild type and the ATG-MO injected embryos at 16 hpf (Fig. 6A–F). Then, in wild type embryos, the boundaries became chevron-shaped and somitic cells were aligned and elongated at 20 hpf, giving rise to fast muscle fibers (Fig. 6G). A more robust accumulation of Fibronectin and phosphorylated-FAK was observed at the boundaries (Fig. 6H, I). The extracellular matrix Laminin is also accumulated at the boundaries at this stage (Fig. 6J) (Crawford et al., 2003). However, in the ATG-MO injected embryos, the boundaries disappeared and the somitic cells did not elongate and showed rounded shapes at 20 hpf (Fig. 6K). Accumulation of Fibronectin, phosphorylated FAK and Laminin was not detected at this stage (Fig. 6L–N). These results suggest that Mys is not required for accumulation of Fibonectin and phosphorylation of FAK and the formation of the morphologically distinct boundaries at the initial stage, but is required for maintenance of the initially formed boundaries.

Abnormalities in the fast and slow muscle morphogenesis in the mys-deficient embryo

We analyzed the morphology of the muscle cells at later stages in the *mys*-deficient embryo. In zebrafish, most somitic cells give rise to long fast muscle fibers that are anchored to the intersegmental boundaries (Stickney et al., 2000). One of our gene trap lines, SAGm11D, contained an insertion near the *myosin heavy chain 3* (*myhc3*) gene (Fig. 7A) and expressed GFP in the myotome similarly to the *myhc3* expression pattern (Fig. 7B, C). In this case, the *gfp* transcript was initiated within the T2KSAG insertion, indicating that the *myhc3* enhancer activated a cryptic promoter on the T2KSAG sequence. In the SAGm11D embryos, fast muscle fibers elongated between the myotome boundaries were clearly visible due to the GFP fluorescence (Fig. 7D). We therefore injected ATG-MO into the SAGm11D embryo. In the injected embryos at 30 hpf, the myotome boundary was not formed and the fast muscle fibers were elongated but showed various shapes and lengths (Figure 7E).

We then analyzed the ATG-MO injected embryo by immunostaining using the S58 antibody that specifically detected slow muscle fibers. In wild type embryos, the slow muscle fibers of uniform lengths, that were elongated between the myotome boundaries, were formed in the lateral surface at 32 hpf (Fig. 7F, G). In the ATG-MO injected embryos at 32 hpf, the slow muscle fibers were formed but showed various shapes and lengths (Fig. 7H). The localization of the slow muscle fibers was also perturbed. Some slow muscle cells were located more medially in deeper areas of the somite (Fig. 7I). The adaxial cells, which are formed adjacent to the notochord and then migrate to the lateral surface, give rise to slow muscle cells (Devoto et al., 1996). We analyzed the adaxial cells in wild type and the ATG-MO injected embryos at 15 hpf, and found that the adaxial cells of normal sizes and positions were formed both in wild type and the injected embryos (Fig. 7J, K), indicating that the *mys*-deficiency does not affect the formation of the adaxial cell.

Immunostaining of the Flag-Mys fusion protein and cell transplantation

We then analyzed the subcellular localization of the Mys protein. We created the Flag-Mys fusion construct and synthesized *flag-mys* mRNA in vitro. When 200 pg of *flag-mys* mRNA was injected into embryos from the *mys* homozygous female, 30 out of 54 embryos (56%) showed normal somite boundaries at 13 hpf, indicating that the fusion protein is functional and can rescue the *mys* mutant phenotype, at least partly. This experiment also showed that injection of the *flag-mys* mRNA itself did not cause any obvious morphological defects. We analyzed the embryos injected with the *flag-mys* mRNA by immunostaining using the anti-Flag antibody. The Flag-Mys protein was detected throughout the cytoplasm of somitic cells at 16 hpf and 20 hpf (Fig. 8A–D). Thus, Mys is likely to function as a cytoplasmic factor and specific subcellular localization was not observed at this level of analysis.

To determine whether the morphological defect observed in the *mys*-deficient cells is autonomous, we transplanted blastomeres of embryos injected with ATG-MO, rhodamine-dextran and *gfp* mRNA into wild type embryos and analyzed the transplanted embryo at 20 hpf. The boundaries were normally formed and the transplanted cells were elongated (Fig. 8E). This result suggested that the *mys*-deficient cells retain ability to elongate and the cell shape was determined non-autonomously, dependently on the shapes of the surrounding cells. Then we transplanted blastomeres of wild type embryos injected with rhodamine-dextran and *gfp* mRNA into ATG-MO injected embryos. In these embryos, the somite boundaries were not maintained and transplanted wild type cells were not elongated and showed rounded shapes at 20 hpf (Fig. 8F). These experiments suggested that the morphological change of the somitic cells was a cell non-autonomous process.

The mys-deficient cells decreased lamellipodia formation on Fibronectin

We found that, although in the *mys*-deficient embryos accumulation of Fibronectin and phosphorylated FAK at the boundaries occurred normally in the initial stage, the subsequent processes were impaired. This observation led us to speculate that Mys is involved in a cellular pathway downstream of the Fibronectin-Integrin signaling. In *Xenopus*, it was shown that cells dissociated from gastrula can form lamellipodia on Fibronectin-coated plastic dishes (Ramos et al., 1996). To test a possibility that the *mys*-deficiency impairs cellular responsiveness to Fibronectin, we developed a cell spreading assay in zebrafish.

First, we placed cells dissociated from wild type embryos at the tail bud stage on Fibronectin-coated slide glasses. We found that the dissociated cells attached to Fibronectin and formed lamellipodia after incubation for overnight at 28 C (data not shown). Since these cells were highly heterogeneous, we then used cells dissociated from wild type embryos at 4 hpf for this analysis. We found that the cells attached to Fibronectin and 73 % of them formed at least one lamellipodium (Fig. 9A and Table 2). We then injected 4 ng of ATG-MO and rhodamine-dextran into the *mys* mutant embryos at the one-cell stage, and collected cells from the injected embryos at 4 hpf. Only 26.7% of the ATG-MO injected cells attached to Fibronectin formed lamellipodia (Fig. 9B and Table 2), indicating that a decreased *mys* activity reduced a cellular activity to form lamellipodia. To analyze whether the Fibronectin-Integrin signaling activated FAK in the ATG-MO injected cells, we performed immunostaining using the anti-phosphorylated FAK antibody. The staining was detected in both wild type and the ATG-MO injected cells after incubation on Fibronectin (Fig. 9C, D, F, G), indicating that FAK was activated in these cells. This staining was not detected in cells immediately after they were placed on the slide glasses (Figures 9E, H). These results indicate that the ATG-MO injected cells are capable of activating FAK in response to Fibronectin signaling.

Discussion

In the present study, our newly designed forward genetics screen for maternal mutants in zebrafish identified a mutation in a novel gene *misty somites* (*mys*). Although vertebrate genomes conservatively contain homologs of the *mys* gene, neither mutations nor functions of the *mys* gene had yet been reported. Furthermore, we discovered that severe knockdown of the *mys* activity caused defective phenotypes in the somite boundary formation which had not been observed by inhibiting the activities of any known factors.

Mys functions as a maternal factor

We observed a pleiotropic phenotype caused by a decreased *mys* activity; i.e., the obscure somite boundary at the 6-somite stage (12–13 hpf), the disappearance of the somite boundary at the 21-somite stage (20 hpf) and the curved body phenotype at 26 hpf. The obscure somite boundary phenotype is caused by a decrease in the maternal *mys* activity since the phenotype was observed in embryos from homozygous mutant females and rescued by either expression of Mys from a transgene or injection of *mys* mRNA. The somite boundary disappearance at 20 hpf is also attributed to the decreased maternal *mys* activity since the phenotype was observed in the ATG-MO injected embryos, but not in the SD-MO injected embryos in which normal splicing of the zygotic *mys* transcript was abolished nearly completely. We carefully examined a possibility that the zygotic *mys* activity also is involved in the somite boundary phenotype by injecting SD-MO into the *mys* mutant embryos. We could not detect any enhancement of the *mys* mutant phenotype. It may seem contradictory that the somite phenotype at 20 hpf was not observed in the *mys* mutant embryos. This may be explained as severer inhibition of the maternal *mys* activity is required to cause the somite boundary disappearance. The zygotic *mys* activity is thought to be responsible for the curved body phenotype since injection of SD-MO solely caused this phenotype. Together, our present study discovered a maternal factor involved in the somite boundary formation, a fairly late event in the embryonic development.

Mys is required for epithelialization of somitic cells

During the somite boundary formation, both Fibronectin and phosphorylated FAK are accumulated at the boundaries, and somitic cells adjacent to the boundaries show epithelial cell characteristics, i.e., a columnar shape and apical localization of the centrosome (Barrios et al., 2003). We found that epithelialization of somitic cells is defective in the *mys*-deficient embryos. This should be a cellular basis for the obscure somite boundary phenotype observed at 12–13 hpf. At 16 hpf, in the *mys*-deficient embryo, the formation of the morphologically distinct boundaries and accumulation of Fibronectin and phosphorylated FAK were observed, but the somitic cells still did not show epithelial cell characteristics. These are in contrast to the *integrinα5* and *fibronectin* mutants in which both accumulation of Fibronectin and phosphorylated FAK, thereby the formation of the distinct boundaries, and epithelialization of the somitic cells were impaired (Julich et al., 2005a; Koshida et al., 2005). From these observations, we speculate that accumulation of Fibronectin at the intersomitic regions may produce signals to induce epithelialization of adjacent somitic cells and the *mys* deficiency interrupted this process. Mys may function in the cytoplasm of the somitic cells and play a crucial role in epithelialization downstream of the Fibronectin signal. Studies are in progress to prove this hypothesis.

Mys is required for maintenance of the somite boundaries

Henry et al. defined three stages of the somite boundary formation, from the initial epithelial boundary to the myotome boundary (Henry et al., 2005). The first stage is the formation of the initial epithelial boundary. Both accumulation of Fibronectin and phosphorylated FAK and epithelialization of somitic cells adjacent to the boundaries occur at this stage show. The second stage is a transition stage. The boundaries become chevron-shaped, and muscle precursor cells

begin to elongate. The third stage is the formation of the myotome boundary. At this stage, all muscle precursors are elongated to generate the myotome. The boundaries formed in the first stage and Fibronectin and phosphorylated FAK accumulated at the boundaries are maintained throughout these stages. Somitogenesis has been studied by forward genetics approaches in zebrafish. The Notch pathway mutants (*aei*, *des*, *mib*, *bea*) and the *fss* mutant (*tbx24*) impaired early segmentation processes (Holley et al., 2000; Holley et al., 2002; Itoh et al., 2003; Nikaido et al., 2002) and the Fibronectin-Integrin pathway mutants (*integrinα5* and *fibronectin*) impaired the formation of the initial epithelial boundary (Julich et al., 2005a; Koshida et al., 2005). All of these defects as well as the *mys* obscure somite boundary phenotype take place before or during the first stage defined by Henry et al. The second *mys* deficiency, the disappearance of the somite boundary, is different from any of these mutant phenotypes since it involves disappearance of the accumulated Fibronectin and phosphorylated FAK at the intersomitic region. Thus, the Mys activity is required to maintain the boundaries during the transition stage. No mutants and genes have been identified that play roles in the transition stage to maintain the somite boundary. We infer that epithelialization of the somitic cells adjacent to the boundaries and signals derived from such cells may be essential for the maintenance of the boundaries formed in the first stage. Studies on the Mys function should give us an insight into molecular mechanisms underlying this process.

Abnormalities in morphogenesis of slow and fast muscle fibers

In the *mys*-deficient embryos at later stages, we observed abnormalities in the morphology of fast and slow muscle fibers, i.e., shapes and lengths of these muscle fibers were aberrant. Since it is thought that the boundaries limit the extent to which muscle cells are elongated (Henry et al., 2005), these abnormalities are likely to be attributed to the absence of the myotome boundary. On the other hand, our observation indicates that the *mys*-deficient fast muscle cells retain capabilities of responding to elongation signals and being elongated. The cell transplantation analysis also supported this notion. It was shown that fast muscle cell elongation is induced by signals from migrating slow muscle cells (Henry and Amacher, 2004). We showed that the adaxial cells, precursors of the slow muscle cells, were normally formed and migrated laterally in the *mys*-deficient embryo although their migration was somehow perturbed. A signal that induced the elongation of the fast muscle cells may have arisen from the slow muscle cells. Or alternatively, it was shown that, even in the *slow-muscle-omitted* mutant that lacked the slow muscle cells, fast muscle cells were elongated (Barresi et al., 2000; Henry and Amacher, 2004). Such a signal may have arisen from other unknown sources.

Role of Mys at the cellular level

In this study, we developed a cell spreading assay in zebrafish. A similar cell spreading assay has been performed in *Xenopus*. In *Xenopus*, cells dissociated from gastrula can attach to Fibronectin and form protrusions, but cells from blastula can attach to Fibronectin but not form protrusions (Ramos et al., 1996). In contrast, we found that cells collected from zebrafish blastula could attach and form protrusions on Fibronectin-coated slide glasses. A mechanism that caused this difference is unknown. We found that the ATG-MO injected cells had a decreased activity to form lamellipodia on Fibronectin, suggesting that Mys is involved in a cellular pathway important for lamellipodia formation. Several cellular factors involved in this process have been described. Cells derived from the FAK-deficient mouse embryo exhibited a rounded cell shape and could poorly spread on Fibronectin-coated dishes (Ilic et al., 1995). The Ena/VASP proteins are accumulated at the tips of lamellipodia and regulate the actin filament networks within lamellipodia (Bear et al., 2002; Rottner et al., 1999). Inhibition of the Ena/VASP function in *Xenopus* cells impaired their ability to form lamellipodia on Fibronectin. In the Ena/VASP-deficient cells, the level of phosphorylated FAK was significantly decreased, suggesting that Ena/VASP and FAK interact either directly or indirectly in lamellipodia formation (Kragtorp and Miller, 2006). In contrast, in the *mys*-

deficient cells, phosphorylated FAK was detected. These may imply that the Mys function is required downstream of or in parallel with the FAK and Ena/VASP pathway.

It is interesting to note that inhibition of either FAK or Ena/VASP causes defects in both spreading on Fibronectin and the somite boundary formation in *Xenopus* (Kragtorp and Miller, 2006). Our present study demonstrated that inhibition of Mys also can cause both defects. A link between lamellipodia formation and the somite boundary formation is totally unknown. The cells' capability to form lamellipodia may play a role during the somite boundary formation. Or alternatively, a cellular pathway required for lamellipodia formation may also be required for epithelialization of the somitic cells and/or the somite boundary maintenance. It will be important to study the Mys function to understand a molecular mechanism underlying these phenomena. The cell spreading assay in zebrafish we described in this study will be a useful method to analyze the cellular function of Mys.

A screen for maternal effect mutants by gene trapping

Maternal effect mutants have been isolated and involvement of maternal factors in the zebrafish development has been discribed (Dosch et al., 2004; Kishimoto et al., 2004; Wagner et al., 2004). Most of the maternal effect mutations manifest their phenotype before the midblastula transition (Dosch et al., 2004; Kishimoto et al., 2004), or are defective in cell viability (Wagner et al., 2004). Several maternal mutations were found to affect the epiboly stage, pattern formation and body plan (Wagner et al., 2004). However, no mutations has been identified that is defective in the somite boundary formation. In this study, we developed a screen to isolate maternal effect mutants using the transposon-mediated gene trap method. The screen for maternal effect mutant by gene trapping has the following advantages. First, maternal expression is easily identifiable by observing GFP expression in one-cell stage embryos and can be prescreened. Second, a female homozygous for an insertion can be identified easily by PCR since the genomic DNA surrounding the insertion can be cloned rapidly. Third, a gene responsible for the mutant phenotype can be identified rapidly by 5′ RACE and RT-PCR. Finally, identification of hypomorphic mutations, such as the *mys* mutation, which should not be easy by a conventional four-generation screen protocol is possible. Our present study demonstrated effectiveness of this approach. We propose that the transposon-mediated gene trap method is powerful to isolate insertional mutations in developmentally important maternal effect genes and zygotic genes as well.

Supplementary Material

Refer to Web version on PubMed Central for supplementary material.

Acknowledgements

We thank S. Takada and S. Koshida for the anti-Fibronectin and anti-phosphorylated FAK antibody and helpful discussion, A. Urasaki and S. Nagayoshi for characterization of the SAG lines, and T. Uematsu, N. Mouri, R. Mimura, M. Mizushina and M. Suzuki for fish works. This work was supported by grants from NIH/NIGM (R01GM069382), the Ministry of Education, Culture, Sports, Science and Technology of Japan, and the Sasakawa Scientific Research Grant from The Japan Science Society.

References

Amsterdam A, Nissen RM, Sun Z, Swindell EC, Farrington S, Hopkins N. Identification of 315 genes essential for early zebrafish development. Proc Natl Acad Sci U S A 2004;101:12792–7. [PubMed: 15256591]

Barresi MJ, Stickney HL, Devoto SH. The zebrafish *slow-muscle-omitted* gene product is required for Hedgehog signal transduction and the development of slow muscle identity. Development 2000;127:2189–99. [PubMed: 10769242]

Barrios A, Poole RJ, Durbin L, Brennan C, Holder N, Wilson SW. Eph/Ephrin signaling regulates the mesenchymal-to-epithelial transition of the paraxial mesoderm during somite morphogenesis. Curr Biol 2003;13:1571–82. [PubMed: 13678588]

Bear JE, Svitkina TM, Krause M, Schafer DA, Loureiro JJ, Strasser GA, Maly IV, Chaga OY, Cooper JA, Borisy GG, Gertler FB. Antagonism between Ena/VASP proteins and actin filament capping regulates fibroblast motility. Cell 2002;109:509–21. [PubMed: 12086607]

Burridge K, Turner CE, Romer LH. Tyrosine phosphorylation of paxillin and pp125FAK accompanies cell adhesion to extracellular matrix: a role in cytoskeletal assembly. J Cell Biol 1992;119:893–903. [PubMed: 1385444]

Crawford BD, Henry CA, Clason TA, Becker AL, Hille MB. Activity and distribution of paxillin, focal adhesion kinase, and cadherin indicate cooperative roles during zebrafish morphogenesis. Mol Biol Cell 2003;14:3065–81. [PubMed: 12925747]

Devoto SH, Melancon E, Eisen JS, Westerfield M. Identification of separate slow and fast muscle precursor cells in vivo, prior to somite formation. Development 1996;122:3371–80. [PubMed: 8951054]

Dosch R, Wagner DS, Mintzer KA, Runke G, Wiemelt AP, Mullins MC. Maternal control of vertebrate development before the midblastula transition: mutants from the zebrafish I. Dev Cell 2004;6:771–80. [PubMed: 15177026]

Driever W, Solnica-Krezel L, Schier AF, Neuhauss SC, Malicki J, Stemple DL, Stainier DY, Zwartkruis F, Abdelilah S, Rangini Z, Belak J, Boggs C. A genetic screen for mutations affecting embryogenesis in zebrafish. Development 1996;123:37–46. [PubMed: 9007227]

Guan JL, Shalloway D. Regulation of focal adhesion-associated protein tyrosine kinase by both cellular adhesion and oncogenic transformation. Nature 1992;358:690–2. [PubMed: 1379699]

Haffter P, Granato M, Brand M, Mullins MC, Hammerschmidt M, Kane DA, Odenthal J, van Eeden FJ, Jiang YJ, Heisenberg CP, Kelsh RN, Furutani-Seiki M, Vogelsang E, Beuchle D, Schach U, Fabian C, Nusslein-Volhard C. The identification of genes with unique and essential functions in the development of the zebrafish, *Danio rerio*. Development 1996;123:1–36. [PubMed: 9007226]

Henry CA, Amacher SL. Zebrafish slow muscle cell migration induces a wave of fast muscle morphogenesis. Dev Cell 2004;7:917–23. [PubMed: 15572133]

Henry CA, Crawford BD, Yan YL, Postlethwait J, Cooper MS, Hille MB. Roles for zebrafish focal adhesion kinase in notochord and somite morphogenesis. Dev Biol 2001;240:474–87. [PubMed: 11784077]

Henry CA, McNulty IM, Durst WA, Munchel SE, Amacher SL. Interactions between muscle fibers and segment boundaries in zebrafish. Dev Biol 2005;287:346–60. [PubMed: 16225858]

Holley SA, Geisler R, Nusslein-Volhard C. Control of *her1* expression during zebrafish somitogenesis by a *delta*-dependent oscillator and an independent wave-front activity. Genes Dev 2000;14:1678–90. [PubMed: 10887161]

Holley SA, Julich D, Rauch GJ, Geisler R, Nusslein-Volhard C. *her1* and the notch pathway function within the oscillator mechanism that regulates zebrafish somitogenesis. Development 2002;129:1175–83. [PubMed: 11874913]

Ilic D, Furuta Y, Kanazawa S, Takeda N, Sobue K, Nakatsuji N, Nomura S, Fujimoto J, Okada M, Yamamoto T. Reduced cell motility and enhanced focal adhesion contact formation in cells from FAK-deficient mice. Nature 1995;377:539–44. [PubMed: 7566154]

Itoh M, Kim CH, Palardy G, Oda T, Jiang YJ, Maust D, Yeo SY, Lorick K, Wright GJ, Ariza-McNaughton L, Weissman AM, Lewis J, Chandrasekharappa SC, Chitnis AB. Mind bomb is a ubiquitin ligase that is essential for efficient activation of Notch signaling by Delta. Dev Cell 2003;4:67–82. [PubMed: 12530964]

Julich D, Geisler R, Holley SA. Integrinα5 and delta/notch signaling have complementary spatiotemporal requirements during zebrafish somitogenesis. Dev Cell 2005a;8:575–86. [PubMed: 15809039]

Julich D, Hwee Lim C, Round J, Nicolaije C, Schroeder J, Davies A, Geisler R, Lewis J, Jiang YJ, Holley SA. *beamter*/*deltaC* and the role of *Notch* ligands in the zebrafish somite segmentation, hindbrain neurogenesis and hypochord differentiation. Dev Biol 2005b;286:391–404. [PubMed: 16125692]

Kawakami K. Transgenesis and gene trap methods in zebrafish by using the *Tol2* transposable element. Methods Cell Biol 2004;77:201–22. [PubMed: 15602913]

Kawakami K. Transposon tools and methods in zebrafish. Dev Dyn 2005;234:244–54. [PubMed: 16110506]

Kawakami K, Koga A, Hori H, Shima A. Excision of the tol2 transposable element of the medaka fish, *Oryzias latipes*, in zebrafish, *Danio rerio*. Gene 1998;225:17–22. [PubMed: 9931412]

Kawakami K, Shima A. Identification of the *Tol2* transposase of the medaka fish *Oryzias latipes* that catalyzes excision of a nonautonomous *Tol2* element in zebrafish *Danio rerio*. Gene 1999;240:239–44. [PubMed: 10564832]

Kawakami K, Shima A, Kawakami N. Identification of a functional transposase of the *Tol2* element, an *Ac*-like element from the Japanese medaka fish, and its transposition in the zebrafish germ lineage. Proc Natl Acad Sci U S A 2000;97:11403–8. [PubMed: 11027340]

Kawakami K, Takeda H, Kawakami N, Kobayashi M, Matsuda N, Mishina M. A transposon-mediated gene trap approach identifies developmentally regulated genes in zebrafish. Dev Cell 2004;7:133–44. [PubMed: 15239961]

Kawamura A, Koshida S, Hijikata H, Sakaguchi T, Kondoh H, Takada S. Zebrafish *hairy/enhancer of split* protein links FGF signaling to cyclic gene expression in the periodic segmentation of somites. Genes Dev 2005;19:1156–61. [PubMed: 15905406]

Keynes RJ, Stern CD. Mechanisms of vertebrate segmentation. Development 1988;103:413–29. [PubMed: 3073078]

Kishimoto Y, Koshida S, Furutani-Seiki M, Kondoh H. Zebrafish maternal-effect mutations causing cytokinesis defect without affecting mitosis or equatorial vasa deposition. Mech Dev 2004;121:79–89. [PubMed: 14706702]

Kishimoto Y, Lee KH, Zon L, Hammerschmidt M, Schulte-Merker S. The molecular nature of zebrafish *swirl*: BMP2 function is essential during early dorsoventral patterning. Development 1997;124:4457–66. [PubMed: 9409664]

Koshida S, Kishimoto Y, Ustumi H, Shimizu T, Furutani-Seiki M, Kondoh H, Takada S. Integrinα5-dependent fibronectin accumulation for maintenance of somite boundaries in zebrafish embryos. Dev Cell 2005;8:587–98. [PubMed: 15809040]

Kotani T, Nagayoshi S, Urasaki A, Kawakami K. Transposon-mediated gene trapping in zebrafish. Methods. 2006

Kragtorp KA, Miller JR. Regulation of somitogenesis by Ena/VASP proteins and FAK during *Xenopus* development. Development 2006;133:685–95. [PubMed: 16421193]

Montero JA, Kilian B, Chan J, Bayliss PE, Heisenberg CP. Phosphoinositide 3-kinase is required for process outgrowth and cell polarization of gastrulating mesendodermal cells. Curr Biol 2003;13:1279–89. [PubMed: 12906787]

Nikaido M, Kawakami A, Sawada A, Furutani-Seiki M, Takeda H, Araki K. *Tbx24*, encoding a T-box protein, is mutated in the zebrafish somite-segmentation mutant *fused somites*. Nat Genet 2002;31:195–9. [PubMed: 12021786]

Pelegri F, Knaut H, Maischein HM, Schulte-Merker S, Nusslein-Volhard C. A mutation in the zebrafish maternal-effect gene nebel affects furrow formation and vasa RNA localization. Curr Biol 1999;9:1431–40. [PubMed: 10607587]

Pourquie O. The segmentation clock: converting embryonic time into spatial pattern. Science 2003;301:328–30. [PubMed: 12869750]

Ramos JW, Whittaker CA, DeSimone DW. Integrin-dependent adhesive activity is spatially controlled by inductive signals at gastrulation. Development 1996;122:2873–83. [PubMed: 8787760]

Reifers F, Bohli H, Walsh EC, Crossley PH, Stainier DY, Brand M. *Fgf8* is mutated in zebrafish *acerebellar* (*ace*) mutants and is required for maintenance of midbrain-hindbrain boundary development and somitogenesis. Development 1998;125:2381–95. [PubMed: 9609821]

Rottner K, Behrendt B, Small JV, Wehland J. VASP dynamics during lamellipodia protrusion. Nat Cell Biol 1999;1:321–2. [PubMed: 10559946]

Sawada A, Fritz A, Jiang YJ, Yamamoto A, Yamasu K, Kuroiwa A, Saga Y, Takeda H. Zebrafish Mesp family genes, *mesp-a* and *mesp-b* are segmentally expressed in the presomitic mesoderm, and Mesp-b confers the anterior identity to the developing somites. Development 2000;127:1691–702. [PubMed: 10725245]

Schulte-Merker S, Ho RK, Herrmann BG, Nusslein-Volhard C. The protein product of the zebrafish homologue of the mouse T gene is expressed in nuclei of the germ ring and the notochord of the early embryo. Development 1992;116:1021–32. [PubMed: 1295726]

Stickney HL, Barresi MJ, Devoto SH. Somite development in zebrafish. Dev Dyn 2000;219:287–303. [PubMed: 11066087]

Urasaki A, Morvan G, Kawakami K. Functional dissection of the *Tol2* transposable element identified the minimal cis-sequence and a highly repetitive sequence in the subterminal region essential for transposition. Genetics 2006;174:639–49. [PubMed: 16959904]

van Eeden FJ, Granato M, Schach U, Brand M, Furutani-Seiki M, Haffter P, Hammerschmidt M, Heisenberg CP, Jiang YJ, Kane DA, Kelsh RN, Mullins MC, Odenthal J, Warga RM, Allende ML, Weinberg ES, Nusslein-Volhard C. Mutations affecting somite formation and patterning in the zebrafish, Danio rerio. Development 1996;123:153–64. [PubMed: 9007237]

Wagner DS, Dosch R, Mintzer KA, Wiemelt AP, Mullins MC. Maternal control of development at the midblastula transition and beyond: mutants from the zebrafish II. Dev Cell 2004;6:781–90. [PubMed: 15177027]

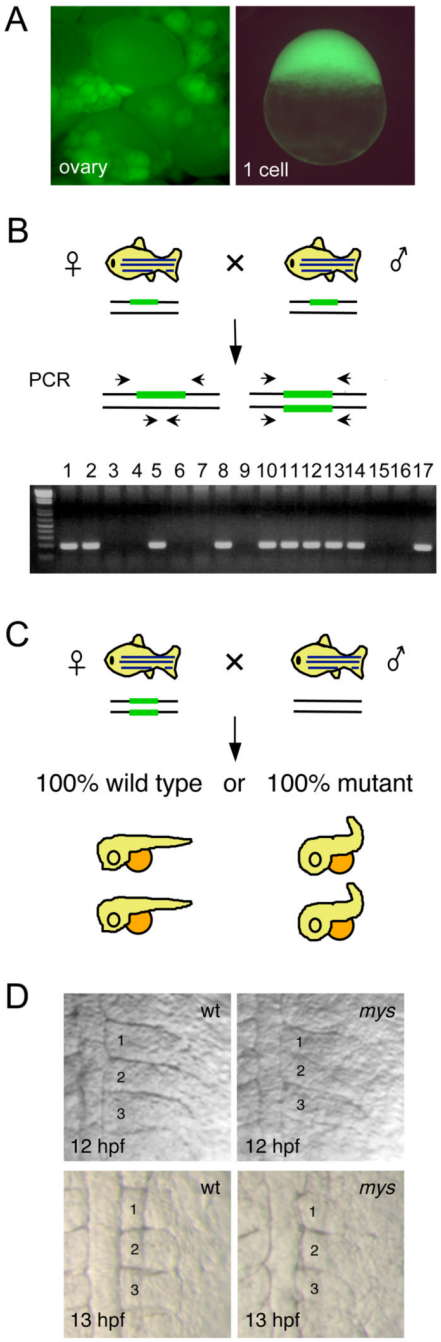

Fig. 1.

A scheme for isolation of maternal effect mutants by transposon-mediated gene trapping. (A) Identification of embryos that express GFP at the one cell stage. GFP expression in the ovary (left) and in fertilized eggs (right) (SAG20A). (B) Identification of fish homozygous for an insertion. Heterozygous male and female fish are crossed and the progeny are analyzed by PCR using primers that locate both sides of the insertion (green bars). The gel is an example of the analysis. A PCR product is amplified from heterozygous fish (lanes 1–2,5,8,10–14 and 17) but not from homozygous fish (lanes 3,4,6,7,9,15 and 16). (C) Homozygous female fish is crossed with wild type male fish and their progeny are analyzed for developmental defects. (D) The somite boundary phenotype at the 3- and 6-somite stages (12 hpf and 13 hpf). (left) Wild type

embryos. (right) Embryos from SAG20A homozygous female fish. Numbers show the somite numbers.

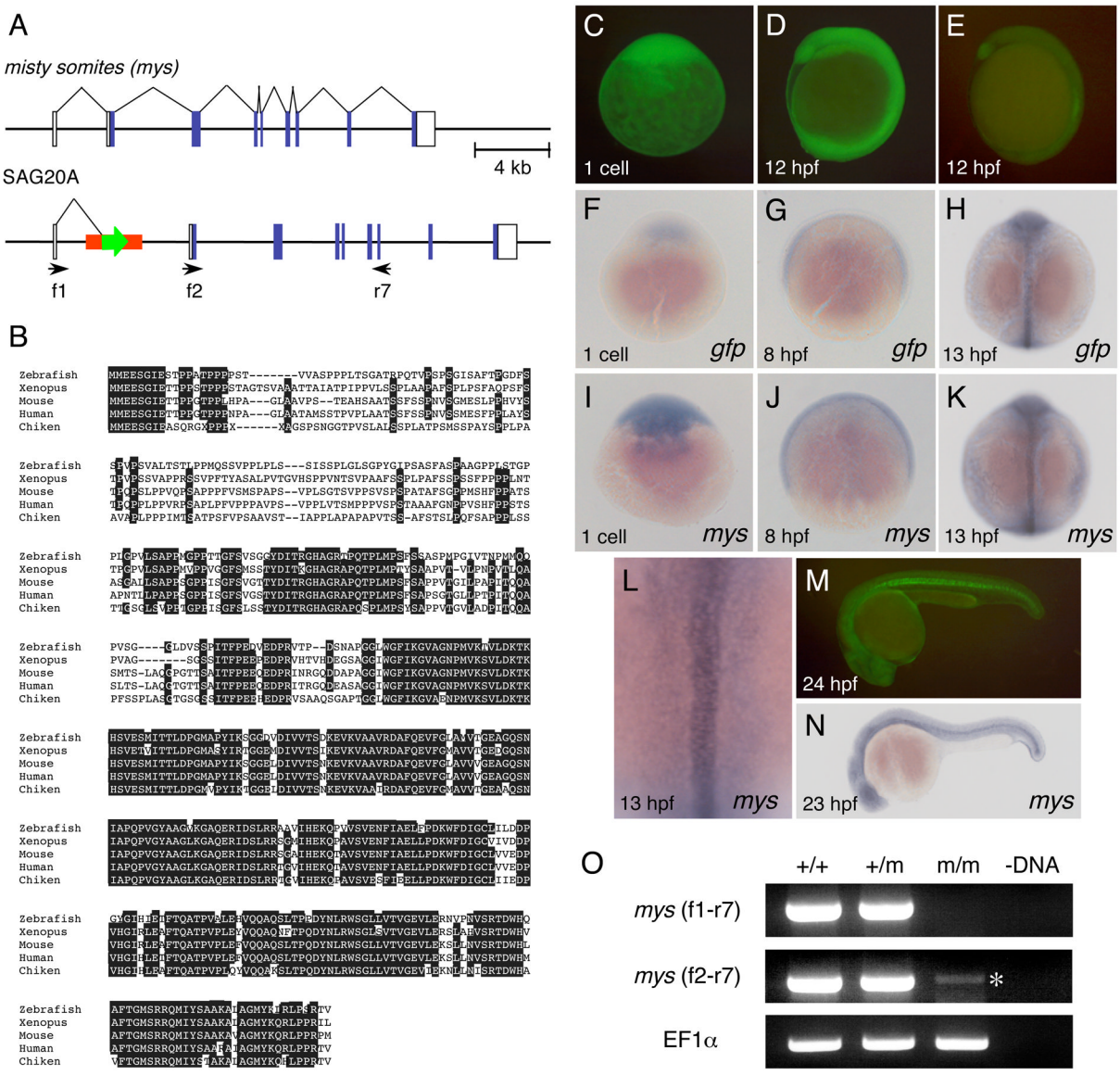

Fig. 2.

Characterization of the SAG20A insertion and the *mys* gene. (A) The structure of the wild type *misty somites* (*mys*) locus and the SAG20A insertion. White boxes indicate untranslated regions and blue boxes indicate coding regions of the *mys* gene. Arrows indicate primers used for RT-PCR. (B) Comparison of the amino acid sequences of the Mys proteins in zebrafish, *Xenopus*, mouse, human and chiken by using ClustalW. Identical amino acids are highlighted in white. (C, D) Maternal GFP expression at the one cell stage (C) and 12 hpf (D). Embryos were obtained from a cross between an SAG20A heterozygous female and a wild type male. The absence of the SAG20A insertion in this embryo was confirmed by PCR at later stages. (E) Zygotic GFP expression at 12 hpf. Embryos were obtained from a cross between an SAG20A heterozygous male and a wild type female. (F–L) In situ hybridization using the *gfp* probe (F–H) and the *mys* probe (I–L). (F) A one-cell stage embryo obtained from a cross between an SAG20A heterozygous female and a wild type male. 8 hpf (G) and 13 hpf (H) embryos obtained from an SAG20A heterozygous male and a wild type female. One-cell stage (I), 8 hpf (J), and 13 hpf (K, L) wild type embryos. *mys* is expressed in the notochord and

weakly and diffusely in the paraxial mesoderm at 13 hpf. (M) Zygotic GFP expression at 24 hpf. Embryos were obtained from a cross between an SAG20A heterozygous male and a wild type female. (N) In situ hybridization of a wild type embryo at 23 hpf using the *gfp* probe. (O) RT-PCR analysis of the *mys* transcript. RNA was prepared from wild type (+/+), heterozygous (+/m) and homozygous embryos (m/m) at 24 hpf and used for cDNA synthesis. (-DNA) A negative control without template DNA. RT-PCR was carried out by using f1 and r7 (top), f2 and r7 (middle), and the EF1 α primers (bottom: positive control). An asterisk indicates a weak transcript with an aberrant start site detected in homozygous embryos.

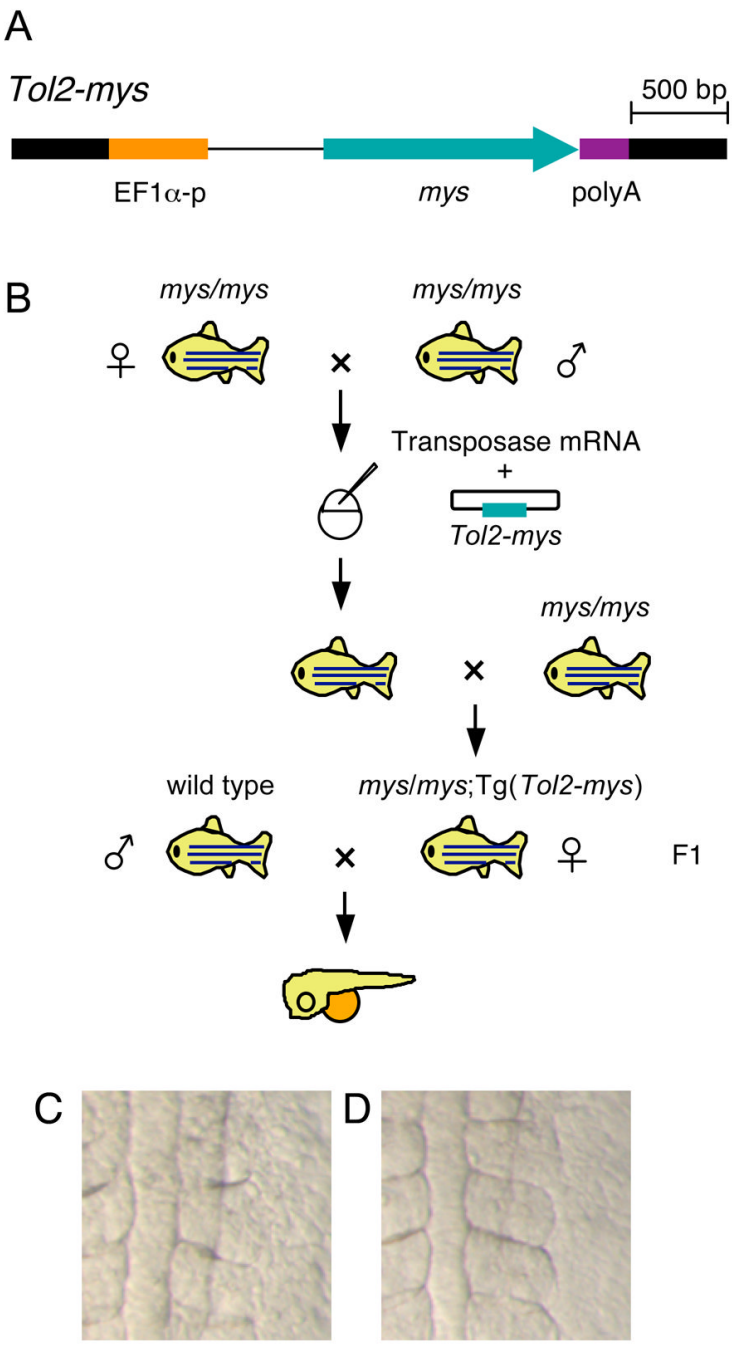

Fig. 3.

Rescue of the *mys* mutant phenotype by transgenesis. (A) The structure of the *Tol2-mys* construct. *mys* cDNA (*mys*) was cloned between the *Xenopus* EF1 α promoter (EF1 α-p) and the SV40 polyA signal (poly A). Thick black lines indicate the *Tol2* sequence. (B) A transposon-donor plasmid containing *Tol2-mys* and the transposase mRNA were co-injected into fertilized eggs produced from *mys* homozygous parents. The injected fish were crossed with *mys* homozygous fish and transgenic fish were identified in the progeny. A female homozygous for the *mys* mutation (*mys*/*mys*) and carrying a single copy insertion of *Tol2-mys* was crossed with a wild type male, and the progeny were analyzed for the phenotype. (C, D) Dorsal views of embryos at the 6-somite stage. (C) Embryos from homozygous (*mys*/

mys) female fish showed the obscure somite boundary phenotype. (D) Embryos from *mys*/*mys*;Tg(*Tol2-mys*) female fish showed distinct somite boundaries.

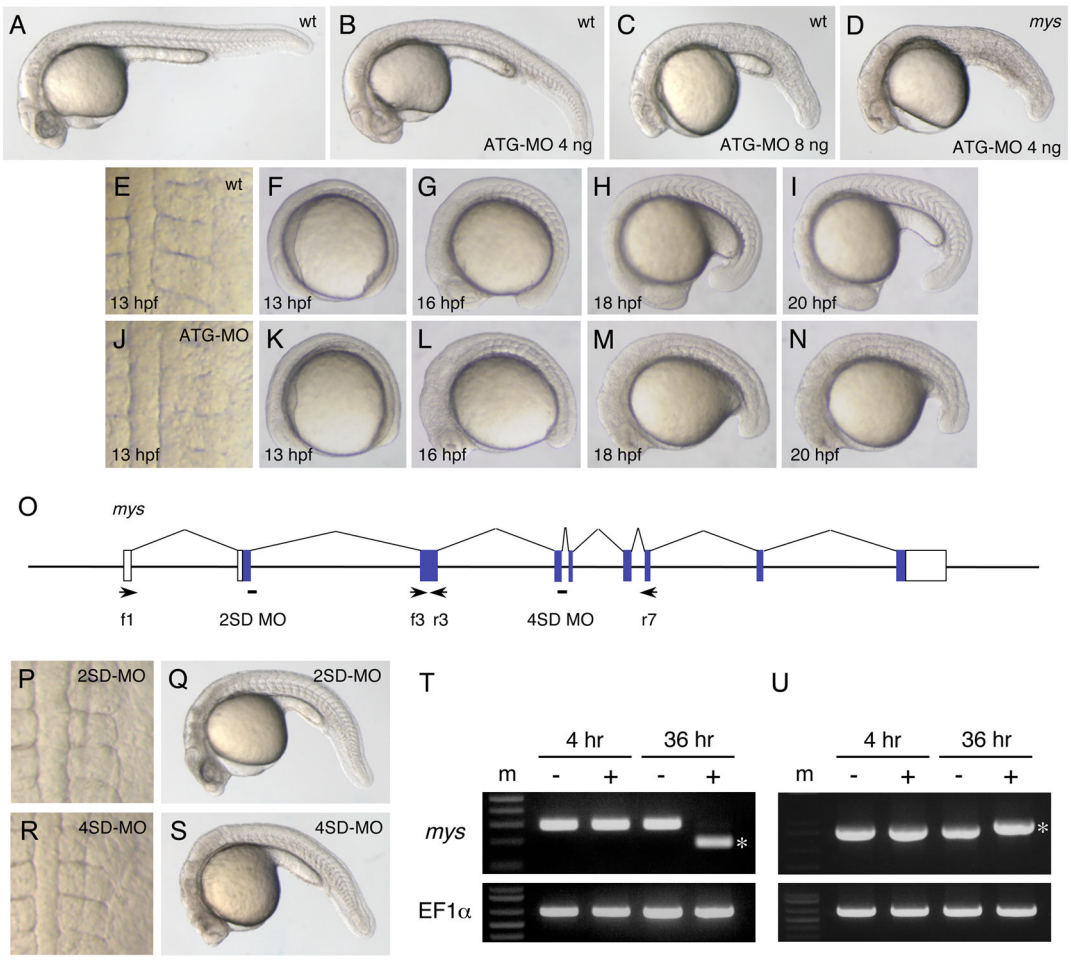

Fig. 4.

Inhibition of the *mys* activity by MO injection caused defects in the somite boundary formation. (A–C) Lateral views of embryos at 26 hpf. (A) A wild type embryo. (B) An ATG-MO injected embryo that showed the curved body phenotype (class I). (C) An ATG-MO injected embryo that showed the curved body and the somite boundary disappearance phenotypes (class II). (D) A *mys* mutant embryo at 26 hpf injected with 4 ng ATG-MO that showed the class II phenotype. (E–I) Dorsal and lateral views of a wild type embryo at 13 to 20 hpf. (J–N) Dorsal and lateral views of an ATG-MO injected embryo at 13 to 20 hpf. In the ATG-MO injected embryo, the obscure somite boundary phenotype is observed at 13 hpf (J), the distinct boundaries are formed at 16 hpf (L) and the boundaries disappear at 18 to 20 hpf (M, N). (O) Positions of 2SD-MO and 4SD-MO and primers. White boxes indicate untranslated regions and blue boxes indicate coding regions of the *mys* transcript. Arrows indicate positions and directions of primers used for RT-PCR. (P, Q) 2SD-MO injected embryos at 13 hpf and 26 hpf. (R, S) 4SD-MO injected embryos at 13 hpf and 26 hpf. The injected embryos showed the curved body phenotype but formed distinct somite boundaries. (T) RT-PCR using f1 and r3 (top) and using the EF1 α primers (bottom). Embryos were injected with H_2O (−) or 2SD-MO (+). RNA was prepared at 4 hpf and 36 hpf. (U) RT-PCR using f3 and r7 (top) and using the EF1 α primers (bottom). Embryos were injected with H_2O (−) or 4SD-MO (+). RNA was prepared at 4 hpf and 36 hpf. Asterisks indicate RT-PCR products of different sizes. SD-MO injection interfered with normal splicing of the zygotic *mys* transcript. (m) DNA size marker.

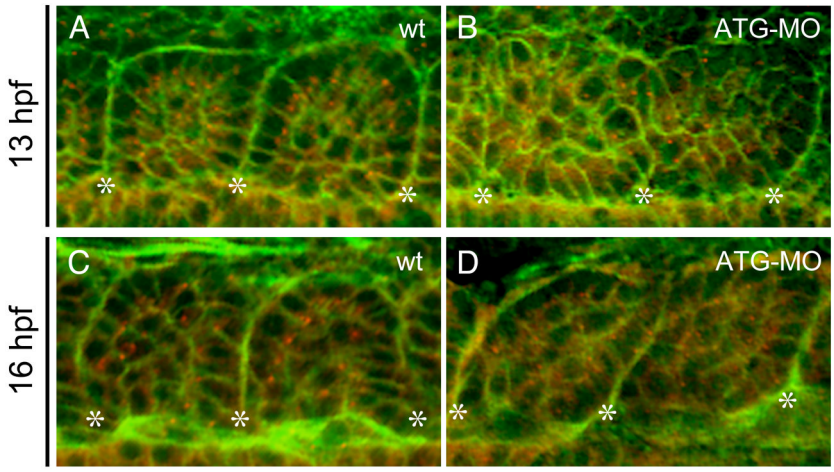

Fig. 5.

The *mys*-deficiency impaired epithelialization of somitic cells. (A–D) Confocal images of embryos stained with the anti-γ-Tubulin antibody (red) and Phalloidin (green). Dorsal views of a wild type embryo (A, C) and an ATG-MO injected embryo (B, D) at 13 hpf (the 6-somite stage) (A, B) or at 16 hpf (the 14-somite stage) (C, D). Asterisks indicate the positions of the somite boundaries. In wild type, somitic cells adjacent to the boundaries show a columnar shape and apical localization of the centrosomes. In the ATG-MO injected embryo, the somitic cells do not show the columnar shape and the centrosomes are distributed randomly in the cytoplasm.

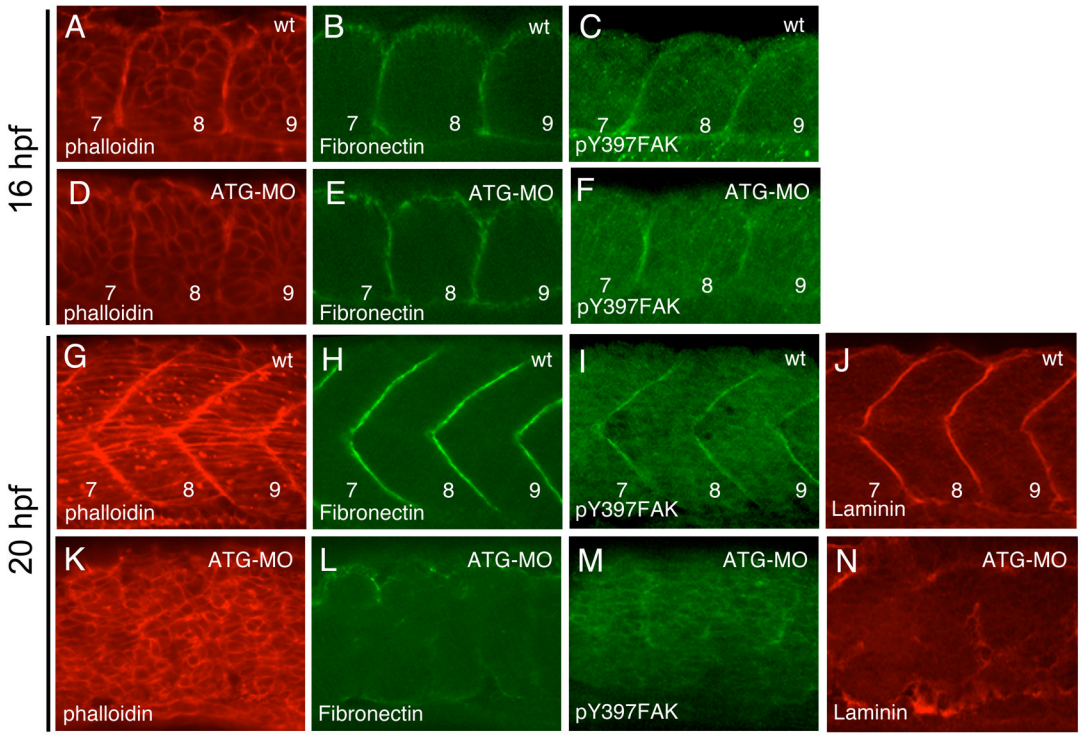

Fig. 6.

Disappearance of the somite boundaries in the *mys*-deficient embryo. Confocal images of wild type (A–C, G–J) and ATG-MO injected embryos (D–F, K–N). (A–F) Dorsal views of the 7th to 9th somite at 16 hpf (the 14-somite stage). (G–N) Lateral views of fast muscle cells of the 7th to 9th somite at 20 hpf (the 21-somite stage). Embryos were stained with phalloidin (A, D, G, K), anti-Fibronectin antibody (B, E, H, L), anti-phosphorylated FAK antibody (C, F, I, M) and anti-Laminin antibody (J, N). Numbers indicate the somite numbers. In the ATG-MO injected embryos, the somite boundaries disappeared at 20 hpf.

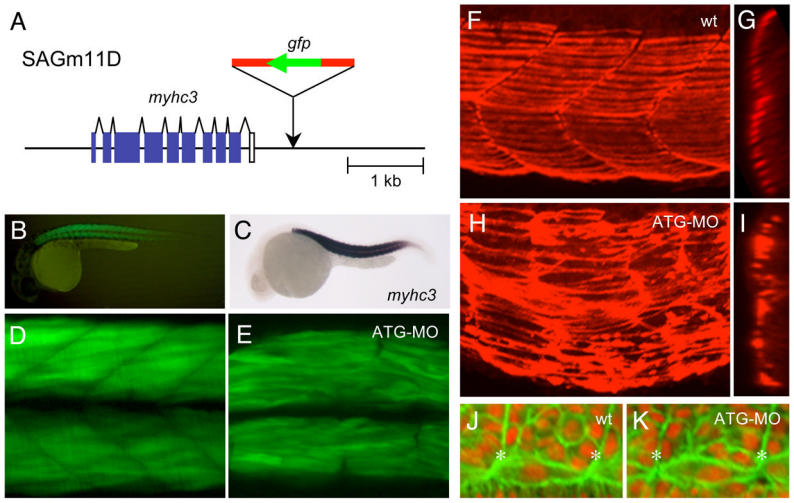

Fig. 7.

Abnormalities in the fast and slow muscle morphogenesis in the ATG-MO injected embryo. (A) The structure of the *myhc3* locus and the SAGm11D insertion. T2KSAG was integrated downstream of the *myhc3* gene. White boxes indicate untranslated regions and blue boxes indicate coding regions. (B) A lateral view of GFP expression in the SAGm11D embryo at 30 hpf. (C) A lateral view of a 24 hpf embryo hybridized with the *myhc3* probe. (D) A confocal image of fast muscle fibers in an SAGm11D embryo at 36 hpf. (E) A confocal image of fast muscle fibers in an SAGm11D embryo injected with ATG-MO at 36 hpf. (F–I) Immunostaining using the S58 antibody that specifically detects slow muscle fibers. Confocal images of a wild type embryo (F, G) and an ATG-MO injected embryo at 32 hpf (H, I). (F, H) Lateral views of the surface area. (G, I) The same samples were rotated on 90 degrees to generate transverse views. (J, K) Confocal images of somitic cells and adaxial cells located adjacent to the notochord. Dorsal views of a wild type embryo (J) and an ATG-MO injected embryo at 15 hpf (K). The notochord is at the bottom. Asterisks indicate the positions of the somite boundaries. The adaxial cells that elongate to span the length of the somite were formed both in wild type and the ATG-MO injected embryos.

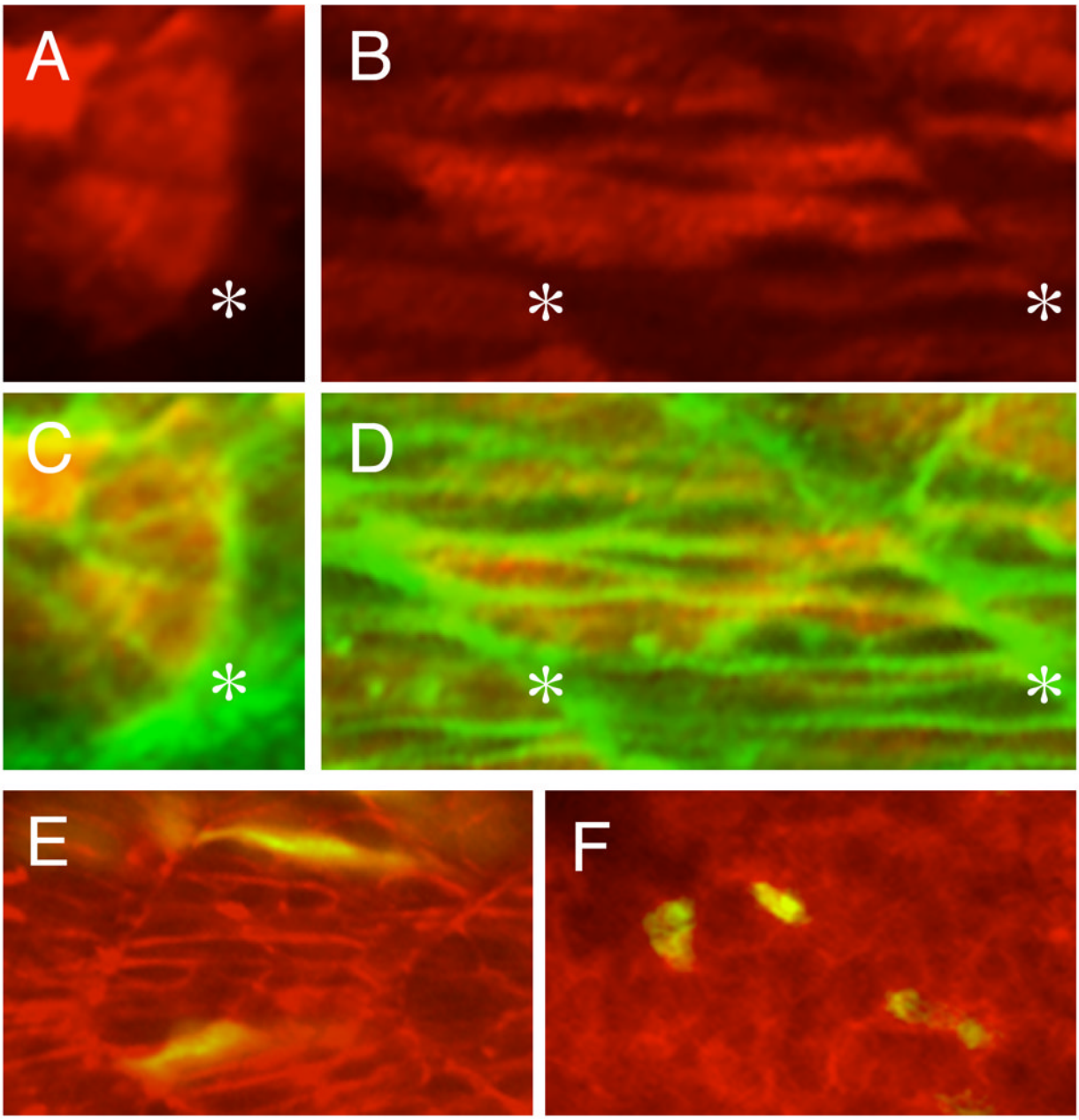

Fig. 8.

Immunostaining of the Flag-Mys fusion protein and cell transpolantation. (A–D) Confocal images of embryos injected with *flag-mys* mRNA and stained with the anti-Flag antibody (red) and Phalloidin (green). (A, C) Dorsal views of the somite at 16 hpf. (B, D) Lateral views of the somite at 20 hpf. (C, D) Merged images. Asterisks indicate the positions of the somite boundaries. The Flag-Mys protein was distributed throughout the cytoplasm. (E, F) Confocal images of lateral views of transplanted embryos at 20 hpf. (E) Cells from embryos injected with ATG-MO, rhodamine-dextran and GFP mRNA were transplanted into a wild type embryo. (F) Cells from embryos injected with rhodamine-dextran and GFP mRNA were transplanted into an ATG-MO injected embryo. The recipient embryos were stained with phalloidin (red) and transplanted cells were labeled in yellow. The ATG-MO injected cells

were elongated in the wild type embryo (E) and the wild type cells showed rounded shapes in the ATG-MO injected embryo.

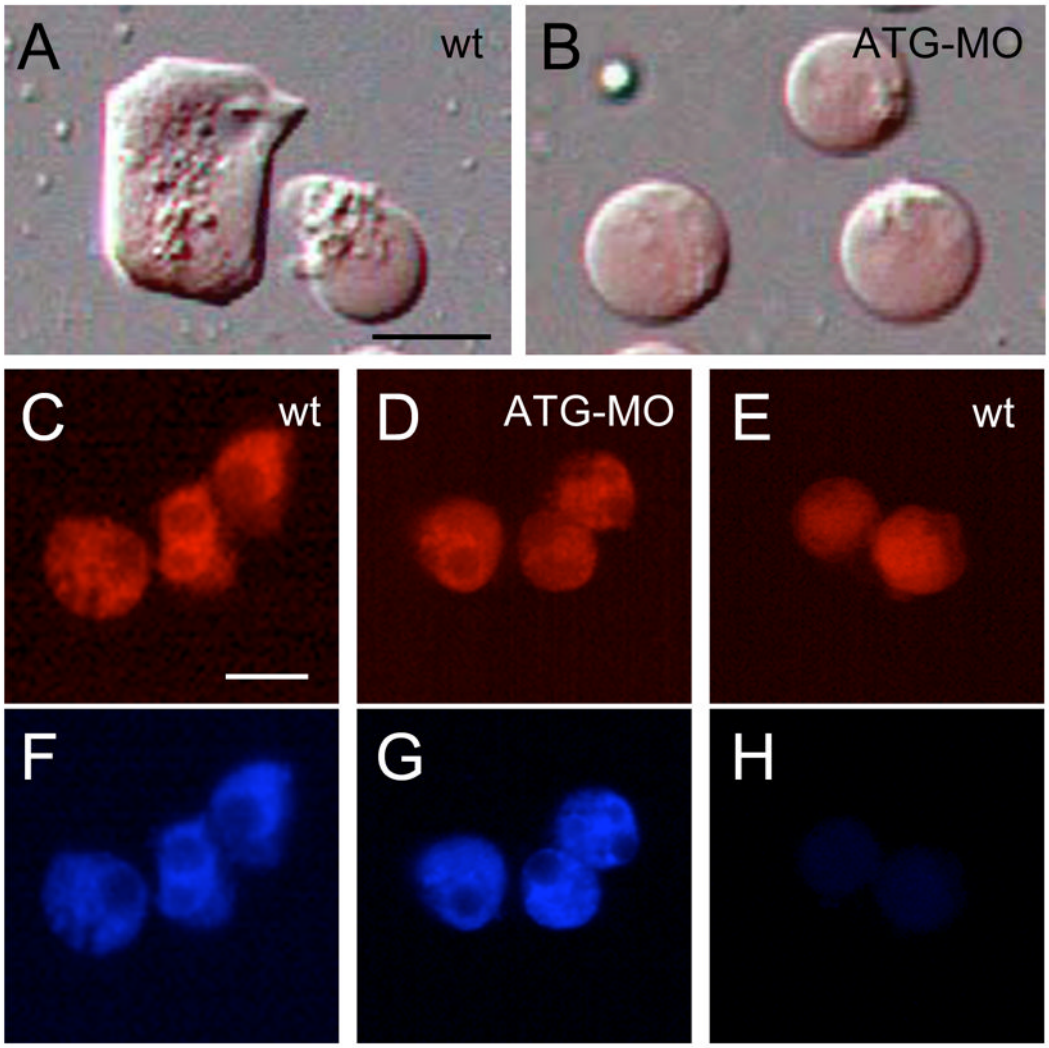

Fig. 9.

The *mys*-deficient cells decreased lamellipodia formation on Fibronectin. (A, B) The morphology of cells dissociated from 4 hpf embryos and incubated on Fibronectin for overnight. (A) Cells dissociated from wild type embryos. (B) Cells dissociated from the ATG-MO injected embryos. The embryos were injected with rhodamine-dextran (red). Lamellipodia formation is impaired in the ATG-MO injected cells. (C–H) Analysis of FAK activation. Wild type cells (C, F) and the ATG-MO injected cells (D, G) incubated on Fibronectin for overnight. (E, H) Wild type cells immediately after placed on Fibronectin. (C, D, E) Images of rhodamine-dextran. (F, G, H) Immunostaining using the anti-phosphorylated FAK antibody. FAK is activated in the ATG-MO injected cells. Scale bars show 20 μm.

Table 1

Injection of ATG-MO into wild type and the *mys* mutant embryos

Embryo	MO	Dose (ng)	n	Phenotype		
				Normal	ClassI	ClassII
wild type	ATG	2	182	84%	16%	0%
		4	236	9%	79%	12%
		8	249	0%	0%	100%
	5-mis	2	116	100%	0%	0%
		4	95	100%	0%	0%
		8	146	100%	0%	0%
mys mutant	ATG	2	243	19%	76%	5%
		4	255	0%	7%	93%
	5-mis	2	112	100%	0%	0%
		4	132	100%	0%	0%

The embryos injected with ATG-MO and 5-mis ATG-MO were classified into three classes by morphological inspection at 26 hpf.

Table 2

Cell spreading assay

Embryo	Number of experiments	Number of cells	Cell morphology	
			Spread	Rounded
wild type	3	1479	73.0% (±7.9)	27.0% (±7.9)
MO-injected	3	1401	26.7% (±6.3)	73.7% (±6.3)

Cells dissociated from wild type embryos and from the embryos injected with ATG-MO and incubated on Fibronectin-coated slide glasses were classified into two groups. Standard deviations are shown in parentheses.